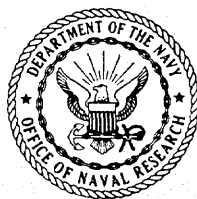# Ionospheric Parameters Derived From Echo II Radar Returns During Solar Minimum Conditions

John M. Goodman

Search Radar Branch
Radar Division

February 21, 1966

U.S. NAVAL RESEARCH LABORATORY
Washington, D.C.

CONTENTS

ABSTRACT

Radar returns from the Echo II satellite (1964-4A) have been analyzed for Faraday rotation effects in order to ascertain their utility in deducing both the subsatellite electron content and the equivalent slab thickness of the daytime ionosphere. These two ionospheric quantities were computed for each satellite transit upon consideration of the Faraday fading phenomenon and the geomagnetic field parameter $H \cos \theta \sec \chi$. The analysis may lead to a possible overestimation of the electron content and slab thickness values, but the degree of overestimation should have only minor bearing on the relative effects. As a result of the present investigation, the following conclusions have been reached:

a. The subsatellite electron content generally exhibits a large variance, but its average value tends to be largest near midday and decreases with increasing solar zenith angle.

b. The daily equivalent slab thickness exhibits no marked variation between 0800 and 1800 EST, although midafternoon values are somewhat in excess of prenoon values.

c. The seasonal equivalent slab thickness has its minimum in local winter and its maximum in local summer; the equinox values are intermediate, with the autumnal equinox exhibiting higher computed values than the vernal equinox period.

d. The mean scale height $\bar{H}_s$ and the mean neutral gas temperature $\bar{T}$ for the ionosphere were found to be 94 km and 1582° K, respectively, during daytime hours. The daytime ionosphere was found to be 500° K warmer in summer than in winter, with the mean equinox temperature being close to the all-season average.

e. No pronounced correlation with Zurich sunspot number of decimetric solar flux was discernible, which was probably due to the fact that statistical variations in the observations exceeded the real variations which might have occurred as a result of solar activity changes.

f. No correlation with the magnetic index K was noted. These conclusions are based on radar echo data obtained during the recent period of minimum solar activity.

PROBLEM STATUS

This is an interim report; work on the problem is continuing.

AUTHORIZATION

NRL Problem R02-05
Project RF 001-02-41-4001

IONOSPHERIC PARAMETERS DERIVED FROM
ECHO II RADAR RETURNS
DURING SOLAR MINIMUM CONDITIONS

INTRODUCTION

Since the advent of artificial earth satellites, numerous studies of the ionosphere have been conducted. These studies have been generally directed toward the determination of the total electron content because spatial inhomogeneities in the ionospheric content are the principal cause of radiowave perturbations. These perturbations include phase and group path variations, polarization rotation, angle-of-arrival variations, absorption, and amplitude scintillations.

The earliest Faraday-rotation studies of the ionosphere were conducted by J. V. Evans [1] utilizing the lunar surface as a reflector of vhf radar pulses. Subsequently, numerous investigators utilized the lunar Faraday-rotation technique to deduce the cis-lunar electron content [2-6]. Kindred analysis of artifical earth satellite data have been accomplished [7-16]. Of particular interest are some determinations of mean ionospheric scale heights made by B. C. Potts [17] using 1962 Transit 4A data. Radar doppler shifts resulting from the motion of the ionosphere have been studied extensively and have also yielded useful information concerning the subsatellite electron content [18-21]. Recently, Garriott et al. [22] have published an excellent study of electron content and ionospheric slab thickness variations for the midlatitude ionosphere.

Radar returns from the Echo II satellite, which were obtained for 31 transits over the Naval Research Laboratory's Randle Cliff radar site during 1964 and 1965, have been analyzed for Faraday rotation. This report concerns the results of the analysis of 27 daytime transits and includes the computation of the total electron content and equivalent slab thickness of the ionosphere. Possible correlation of the results with geophysical, solar, and ionospheric data is also discussed.

PROCEDURE

Experimental

For 31 transits of the polar-orbiting Echo II satellite (1964-4A) over Chesapeake Beach, Maryland, during the recent epoch of sunspot minimum activity (viz., 1964 and 1965), chart recordings of radar returns were obtained. Vertically polarized signals were transmitted and both horizontal and vertical polarizations were received. The nominal radar characteristics are listed in Table 1.

The Echo II satellite was in a polar orbit and its average inclination, apogee, and perigee during the 14 months of sporadic observations were 81.5°, 1239 km, and 1062 km, respectively. The minimum perigee was approximately 1000 km, which is normally* above about 98 percent of the total content of ionospheric electrons. Satellite ephemerides and approximate coordinates in the local horizon system for the Randle Cliff radar

---

*Normal conditions in this report imply that the daytime ionosphere is Chapman-distributed with a neutral scale height of 100 km and that the altitude of the $F2$ maximum is 300 km.

Table 1
Nominal Characteristics of NRL's
Randle Cliff Radar

Parameter	Value
Frequency (Mc/s)	138.6
Pulse Power (kw)	375
Pulse Length (μsec)	100
Antenna Gain (db)	34.6
Antenna Beamwidth (degrees)	3.6
Receiver Noise Temperature (°K)	440
Transmitting Losses (db)	0.3
Receiving Losses (db)	1.1
Receiver Bandwidth (kc/s)	23

site (latitude 38° 39.62', longitude 76° 32.15') were furnished by the U.S. Navy Space Surveillance System (NAVSPASUR) and were used to establish radar contact with the target. Upon target acquisition, the Randle Cliff radar was operated in an automatic tracking mode for the majority of transits. Due to the Faraday effect, which resulted in alternate fading in the vertical and horizontal receiver channels, the vertically polarized monopulse tracking system was naturally troublesome, especially when target amplitude scintillation effects were severe. For this reason the less accurate manual tracking mode was sometimes employed.

Analytical

Radar data was initially recorded on magnetic tape, as well as on chart paper, in the hope that fine-scale ionospheric inhomogeneities could be detected upon examination of the pulse-to-pulse data. Due to the apparent wrinkled surface of the satellite, which has a theoretical cross section of 1330 square meters, severe amplitude modulations hampered the fine-scale polarization studies. Radar studies of Echo II conducted by Leavitt et al. (23) at 2300 Mc/s late in 1964 indicated that the surface of the satellite was quite irregular at that frequency. Figure 1 is a typical plot of the pulse-to-pulse radar data obtained by the Randle Cliff radar at 138.6 Mc/s. Upon inspection of the smoothed data (indicated by the curves drawn through the data points) in the horizontal and vertical polarization channels, the existence of a slow Faraday rotation is apparent. This rotation results from the presence of a quasi-smooth ionosphere and a smoothly varying magnetic field parameter (24). Large fluctuations in the modulus of the electric vector may also be evidenced and are presumably caused by variations in the target radar cross section.

Figure 2 illustrates the two major causes of signal fading, viz., Faraday rotation and amplitude scintillation. The Faraday rotation is manifested in two distinct forms. The relatively slow Faraday fading of high amplitude is the most obvious and has been alluded to previously. A low-amplitude Faraday fading component also exists and is caused by ionospheric inhomogeneities. The amplitude scintillation itself may be either real or apparent. Real scintillation effects result from target cross-sectional variations and ionospheric diffraction. Apparent scintillation may be a result of numerous causes,
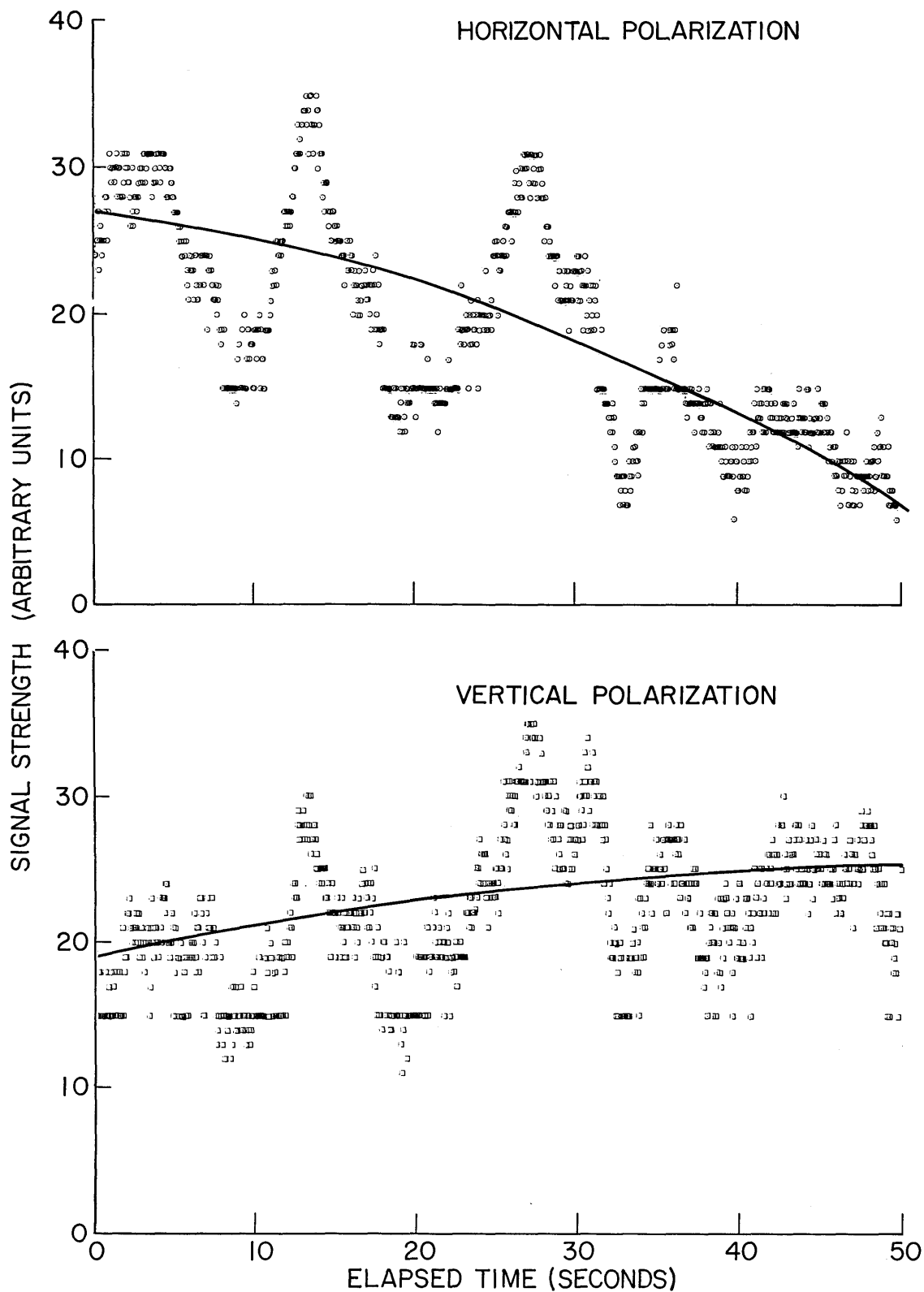
Fig. 1 - Signal strength as a function of time on a pulse-to-pulse basis
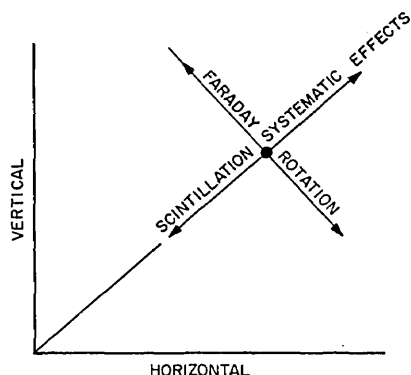for vertical and horizontal polarizations at 138.6 Mc/s

Fig. 2 - The effect of system-
atic changes, scintillation, and
Faraday rotation on the signal
strength of horizontal and ver-
tical polarizations

including tracking irregularities, receiver gain
changes, and transmitter pulse power variations.
The magnitude of the apparent scintillations was
found to be negligible in those regions for which
tracking problems did not arise.

Ionospheric diffraction gives rise to signal
scintillation, but the well-established diurnal
dependence of the ionospheric scintillation effects
was not observed. The rate and magnitude of the
observed scintillations appeared to be independent
of the time of day, which suggests that the origin of
the disturbance was not ionospheric diffraction.
Consequently, for those regions in which system-
atic fluctuations may be considered negligible, the
low- and high-frequency Faraday fading effects and
target cross-sectional variations generate all
signal perturbations. Due to the low magnitude of
the high-frequency Faraday fading (Faraday noise),
this fading interferes with the cross-sectional
scintillation, and, as a consequence, the measured
effects are not easily traced to the proper causes. It was concluded that the smoothed
records of Faraday fading, being representative of a quasi-smooth ionosphere, could
still be salvaged for determinations of the average values of the subsatellite electron
content and the equivalent slab thickness of the ionosphere.

Those chart recordings of the radar returns which exhibited at least one discernible
fade ($\pi/2$ radians) were considered suitable for analysis. The pertinent magnetic field
data was extrapolated from the surface projection of the weighted ionospheric mean
(or ionospheric point), which was assumed to be located at a nominal altitude of 400 km.
The determination of the geomagnetic field parameter $\bar{\psi}$ has been discussed in NRL
Report 6234 (24). Figure 3 is a plot of $\bar{\psi}$ for an altitude of 400 km referenced to the
Randle Cliff site as a function of the azimuth angle A, with the elevation angle ϵ as a
parameter. Since Echo II is a polar-orbiting satellite, the function $\bar{\psi}$ is always at least
a monotonic function of time and, in most cases, it is either strictly increasing or
strictly decreasing. With the function $\bar{\psi}$ (A, ϵ) adequately defined, Faraday fade angles
derived from the recordings were translated into single smoothed values of the subsatel-
lite electron content C for each transit by means of the following simple formula which
results from the monotonicity of $\bar{\psi}$:

$$C = \int_0^{h_t} N \ dh = 3.22 \times 10^{17} \left(\frac{\Delta\Omega}{\bar{\psi}_2 - \bar{\psi}_1} \right), \text{ (mks units)} \tag{1}$$

where $\Delta\Omega$ represents the total fade angle in radians during the period of observation,
N is the electron density at an altitude h, and $\bar{\psi}_1$ and $\bar{\psi}_2$ are the initial and terminal
values of the magnetic field parameter. Four standard and reasonably justifiable
assumptions are embodied in Eq. (1):

    a. a quasi-longitudinal propagation mode exists
    b. negligible path bending occurs
    c. negligible path splitting occurs
    d. the high-frequency approximation is valid.

At 138.6 Mc/s the listed assumptions are generally accurate and their invocation does not
generate measurable errors in the computation; however, a fifth assumption is also
incorporated into the derivation of Eq. (1), namely, that of spherical stratification. This

assumption is necessary in order to avoid the nπ rotational ambiguity, but its validity is questionable in some instances.
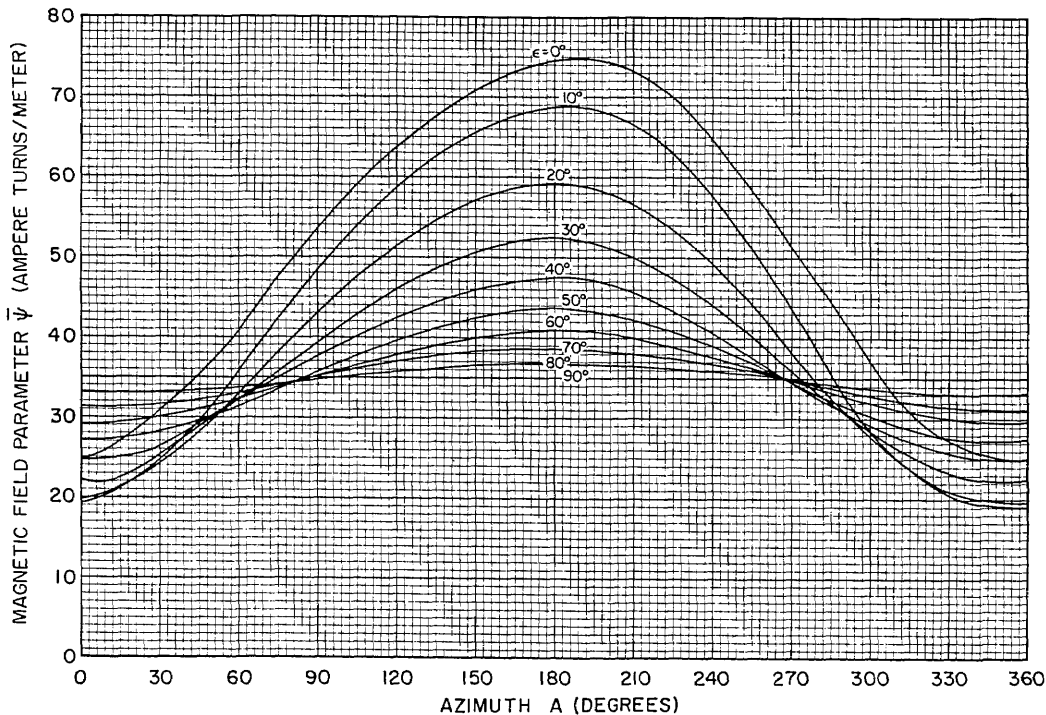

Fig. 3 - Magnetic field parameter $\bar{\psi}$ vs azimuth angle A referenced to an altitude of 400 km for the Randle Cliff radar site. The elevation angle ϵ is given as a parameter.

RESULTS AND DISCUSSION

Table 2 is a compilation of the data corresponding to each processed Echo II daytime transit. The complete study included an examination of the possible correlation of electron content and slab thickness variations with ionospheric and solar data and geophysical phenomena. In the simplified analysis, the parameter which was used as the gross ionospheric behavioral indicator was the $F2$-region critical frequency $foF2$. Two indicators of the intensity of ionizing solar radiation were considered, the Ottawa 2800 Mc/s solar flux S and the Zurich sunspot number R_z. The planetary magnetic index K_p represents the relative worldwide magnetic activity, and the sum of eight 3-hourly values

$$\sum_{p=1}^{8} K_p$$

for the date of transit was used for correlation purposes.

The change in the magnetic field parameter when plotted against the total Faraday fade angle should exhibit a general linearity with an average slope proportional to the average content and with a y intercept tending toward zero. From Fig. 4 it is seen that

Table 2
Data for Echo II Daytime Transits

Date	Time (EST)	Var. in Mag. Field Parameter $\Delta\bar{\psi}$ (Ampere turns/m)	Total Fade Angle $\Delta\bar{\Omega}$ (degrees)	Electron Content C (m^{-2})	Critical Frequency f_oF2 (Mc/s)	Equiv. Slab Thickness τ (km)	Zurich Sunspot No. R_z	Solar Flux s	Planetary Mag. Index K_p
5-1-64	1146	17.5	180	5.8×10^{16}	4.5	231	7	68.9	27-
6-17-64	1356	20	450	12.7	5.7	382	11	71.5	7+
6-19-64	1145	40	990	13.9	4.8	488	23	70.1	9-
6-23-64	1150	42	900	12.1	5.0	390	0	67.4	13o
9-22-64	1446	35	540	8.7	5.2	259	0	68.7	29o
9-24-64	1204	16.5	450	15.4	6.0	349	0	68.0	17-
9-24-64	1447	12	360	16.9	5.5	452	0	68.0	17-
9-27-64	1139	26	540	11.7	5.4	323	0	69.7	9o
9-28-64	1350	18	630	19.7	4.5	806	0	70.2	35-
9-28-64	1705	16	360	12.7	4.6	482	0	70.2	35-
9-29-64	1328	21	450	12.1	5.5	326	0	70.7	13o
10-2-64	1208	5.5	90	9.2	5.4	255	11	71.5	8-
10-2-64	1356	20	450	12.7	5.7	382	11	71.5	8-
12-8-64	1426	20	540	15.2	6.0	341	8	77.3	12-
1-6-65	1140	44.1	900	11.5	6.2	241	19	80.4	4-
1-6-65	1320	11.5	360	17.6	6.6	319	19	80.4	4-
1-25-65	0956	37	510	7.8	5.3	222	21	75.5	3+
1-26-65	0922	19	450	13.3	5.4	370	21	75.9	3+
1-26-65	1113	26	630	13.6	5.2	407	21	75.9	3+
4-5-65	1438	20	540	15.2	5.9	352	0	70.8	6+
4-12-65	1448	36	990	15.5	5.7	385	0	71.1	13+
4-27-65	1047	9	180	11.3	5.0	343	10	69.2	10-
5-18-65	0856	20	450	12.7	5.3	365	11	70.4	8-
6-11-65	0716	34	540	8.9	3.5	591	7	76.5	9o
6-17-65	1529	29	540	10.5	5.0	338	12	76.3	32o
7-1-65	1332	21	630	17.0	5.0	527	18	76	*
7-1-65	1523	35	1080	17.4	5.1	518	18	76	*

* Not available at time of writing.

this is indeed the case, although some variance from linearity due to electron content variations is obviously present. Since $\Omega \sim \bar{\psi} C$, we have

$$\Omega_2 - \Omega_1 \sim C_2 \left[\bar{\psi}_2 - \bar{\psi}_1 \left(C_1 / C_2 \right) \right]. \tag{2}$$

The prevailing linearity must have resulted from two factors:

a. $\left(\Omega_2 - \Omega_1 \right) \sim \left(\bar{\psi}_2 - \bar{\psi}_1 \right)$, and

b. the observed values of content were independent of the number $\bar{\psi}_2 - \bar{\psi}_1$ and the observed variance in content was a constant function of $\bar{\psi}_2 - \bar{\psi}_1$, which add credence to the argument that spherical stratification is roughly approximated in the ionosphere. The overall mean content was observed to be 1.3×10^{17} electrons-m^{-2}, and the ratio of maximum to minimum observed values was 3.4:1.
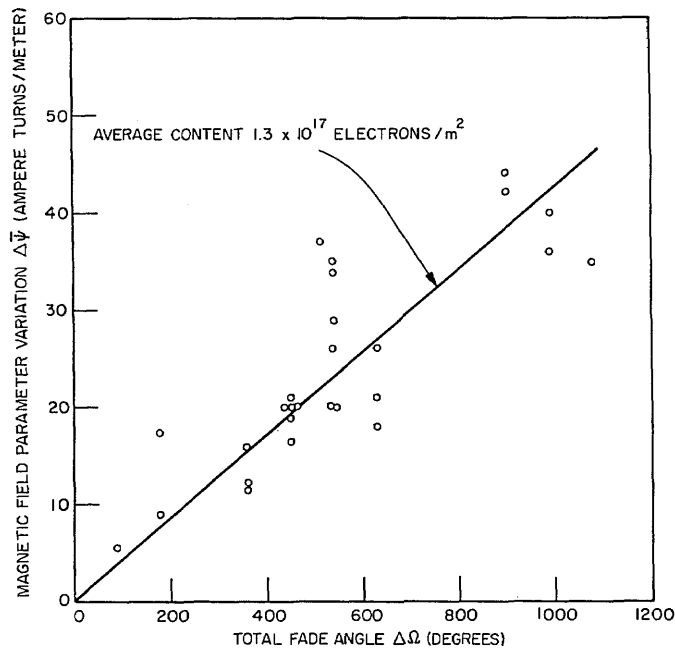

Fig. 4 – Magnetic field parameter variations $\Delta \bar{\psi}$ as a function of the observed rotational changes (fade angle) $\Delta \Omega$. The slope of the line drawn from the origin to any data point defines the electron content associated with that data point.

A plot of the subsatellite electron content C vs the peak $F2$-region density $NF2$ is given in Fig. 5. The plot suggests that electron content is an increasing function of the peak density $NF2$. The observed deviations from a mean slab thickness of 387 km imply that the daytime ionosphere does not have a consistent shape. The variance which the daytime ionosphere exhibits both in total content and in equivalent slab thickness may be seen upon inspection of Figs. 6 and 7. Aside from the scatter of the data points, it is apparent that the electron content is generally highest near midday and decreases with increasing solar zenith angle. The daytime slab thickness has no significant structural feature, although afternoon values tend to be somewhat larger than prenoon values. Figures 8 and 9 illustrate the dependence of slab thickness upon 2800-Mc/s flux S and Zurich sunspot number R_z, respectively. Unfortunately, during the days in which

observations were made, no significant excursions in solar flux or sunspot activity occurred; however, over the small activity excursion range available, a slight inverse correlation of slab thickness with increasing values of S and R_z is noticed. This effect might be more apparent than real because the statistical variations in slab thickness would be expected to dominate real variations if minor changes in S and R_z are involved. The fact that Garriott et al. (22) have discerned a positive correlation of solar activity with slab thickness for $40 \leq R_z \leq 180$ amplifies the argument that any observed correlation for low sunspot number is an unavoidable manifestation of the statistics. It must be concluded that for low mean sunspot number, the slab thickness dependence upon solar activity excursion is not clear.
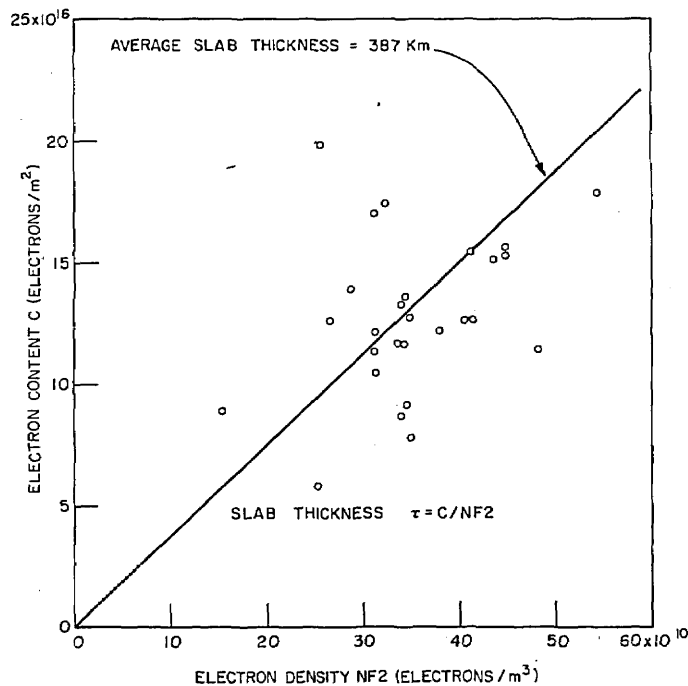

Fig. 5 - Electron content C as a function of maximum $F2$-region electron density $NF2$ as determined by Ft. Belvoir vertical incidence ionosonde

For a Chapman distribution of the ionosphere, the equivalent slab thickness τ is directly proportional to the neutral-particle scale height $H_s = kT/Mg$, where k is Boltzmann's constant, T is the mean absolute temperature, M is the mean molecular weight, and g is the mean value of the gravitational acceleration. Assuming a mean molecular weight of 16 and a mean gravitational altitude of 400 km, we find that

$$H_s = 0.0594\,T, \tag{3}$$

where H_s is in kilometers and T is in degrees Kelvin. By numerical integration of the Chapman function, it may be found that (24)

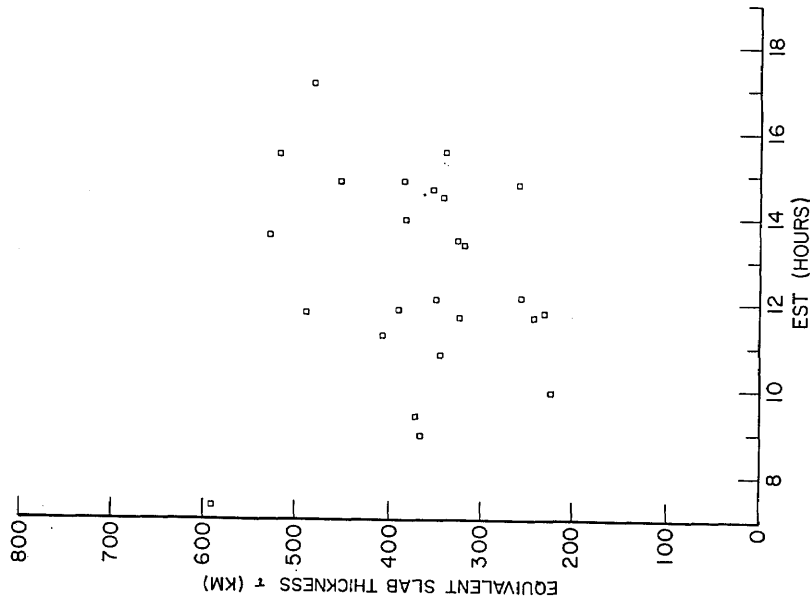$$\tau = a + b\,(H_s - 70), \tag{4}$$

Fig. 7 - Equivalent slab thickness τ of the iono-sphere as a function of Eastern Standard Time (EST). The equivalent slab thickness τ is defined to be the quotient $C/NF2$, where C is the total electron content and $NF2$ is the peak $F2$-region electron density.
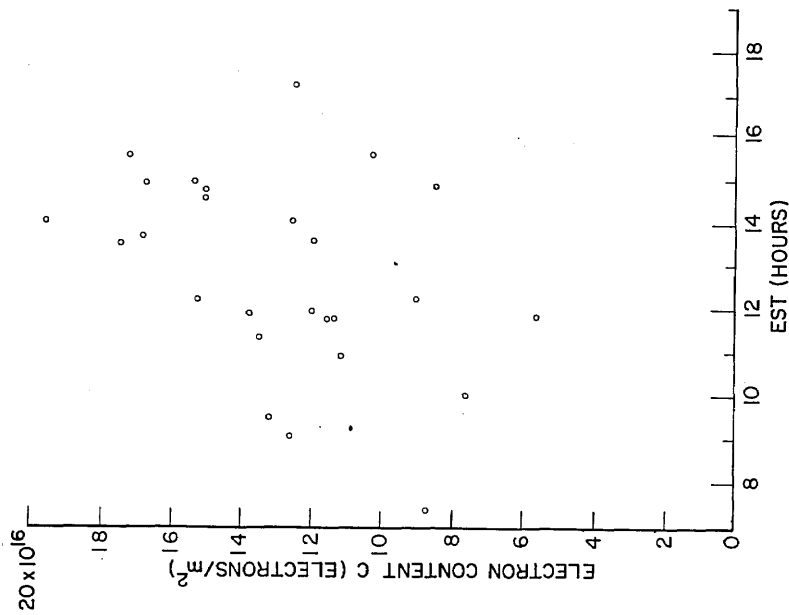

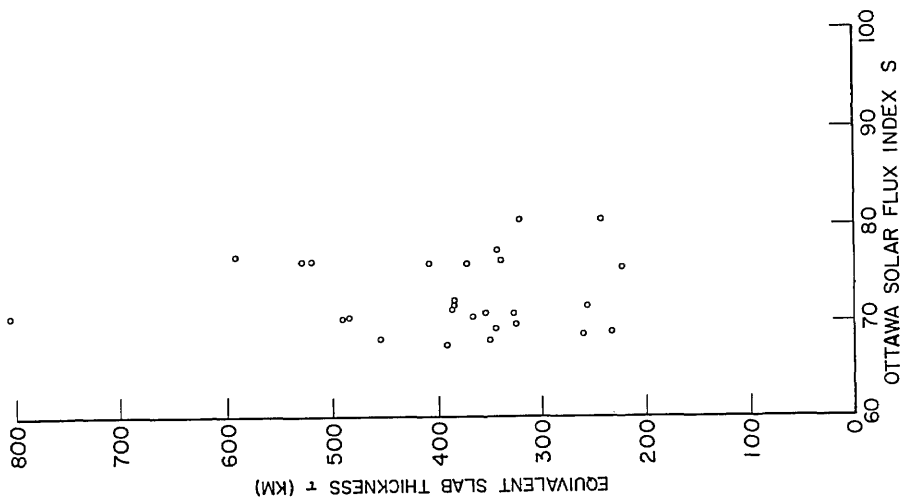Fig. 6 - Electron content C of the ionosphere as a function of Eastern Standard Time (EST)

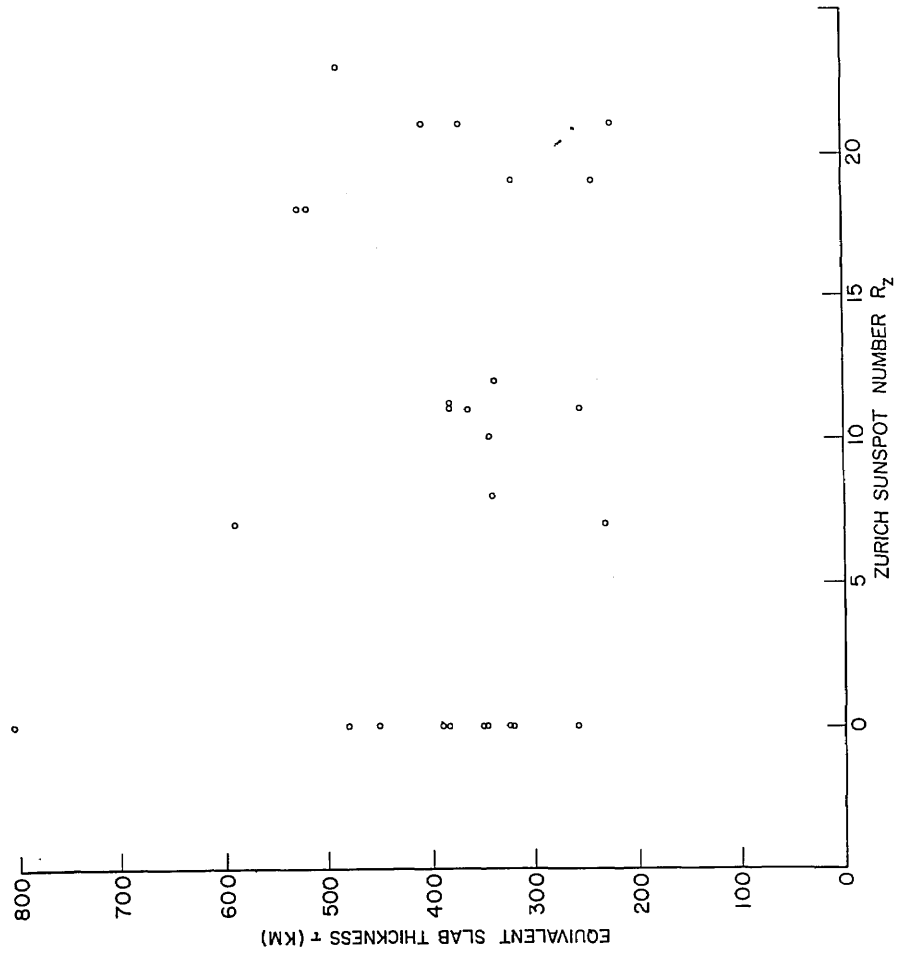Fig. 9 – Equivalent slab thickness τ of the ionosphere as a function of
Zurich sunspot number R_z

Fig. 8 – Equivalent slab thickness τ
of the ionosphere as a function of
Ottawa solar flux S

where a is the effective slab thickness at $H_s = 70$ km and b is the slope. The parameters a and b are both functions of satellite altitude with respect to the $F2$ maximum and are presented in Fig. 10. For superionospheric satellites it may be shown that $\tau \rightarrow 0$ as $H_s \rightarrow 0$, and Eq. 4 may be rewritten more simply as

$$\tau = 4.13 \; H_s \quad (= 0.245 \; T \,). \tag{5}$$

The execution of the necessary translations may be expedited through use of the curves in Fig. 11.
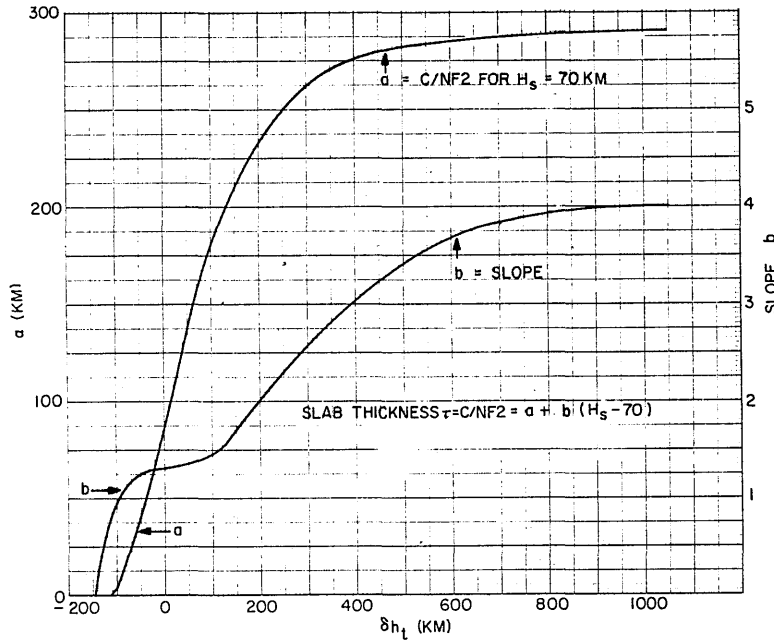

Fig. 10 - Curves from which the slab thickness τ is obtained as a function of the target altitude. The quantity δh_t is equal to $h - h\ F2$.

Some rather interesting facts emerge if the data points are partitioned such that separate seasonal averages may be obtained. For instance, it is seen that the mean values of slab thickness $\overline{\tau}$, scale height $\overline{H}_s$, and neutral gas temperature $\overline{T}$ decrease from summer to winter. Figure 12 is a plot of $\overline{\tau}$, $\overline{H}_s$, and $\overline{T}$ as a function of season. It must be pointed out that T represents the neutral gas temperature for equilibrium conditions, and in the event that equilibrium does not exist, T represents the mean electron-ion temperature. The likely regions for nonvalidity of the equilibrium assumption are at sunrise and sunset. In view of the fact that the data being presented in this report is extracted from daytime observations, the deviation from equilibrium is relatively small with respect to the expected accuracy of the computations. On the average, the ionosphere is about $500°$ "warmer" and 126 km "thicker" in summer than in winter. The scale height increases from a wintertime low of 77 km to a summertime peak of 107 km and the all-season average of the observations was 94 km. It is interesting to note that Seddon's model of the quiet midlatitude ionosphere is one in which the daytime scale height is of the order of 100 km (25). Upon examination of Table 2, which is a numerical listing of the computations, one observes that the autumnal equinox is both "warmer" and "thicker" than the vernal equinox, indicating that the ionosphere is slow
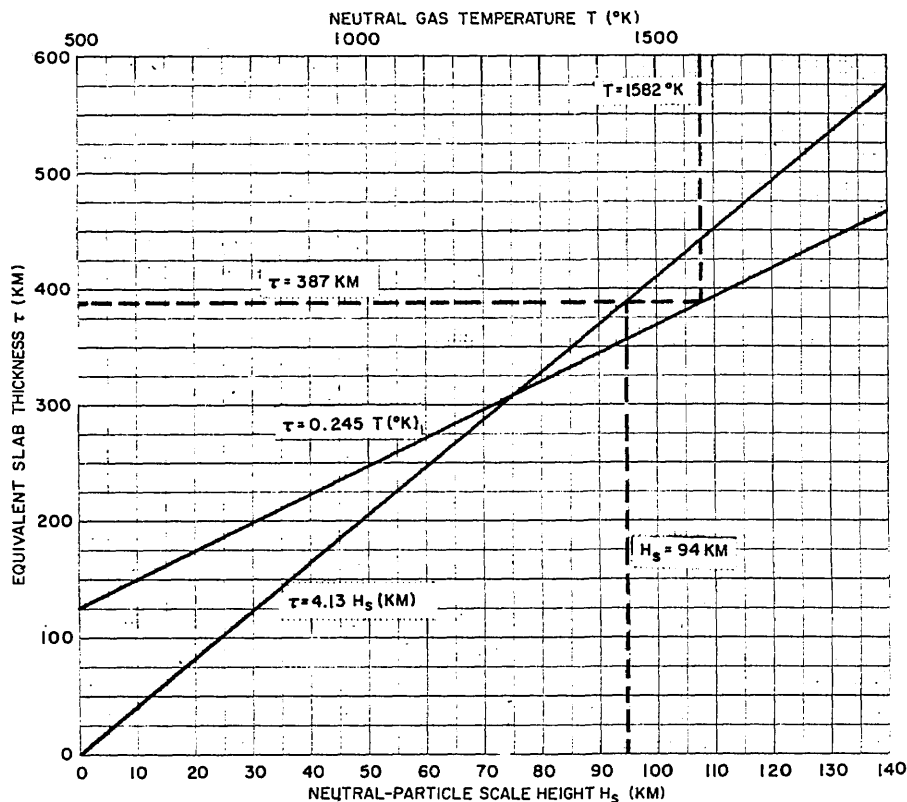
Fig. 11 - Relationships between equivalent slab thickness
τ, neutral-particle scale length H_s, and neutral gas tem-
perature T. The dashed lines indicate how the graph is
to be used.

to lose energy between summer and autumn and relatively quick to gain energy between
spring and summer. Of course, this deduction is based upon data which possess large
probable errors resulting from the small number of observations. Upon consideration
of the probable errors involved, objectively suggests that one must look at answers
qualitatively, even though the numbers are very interesting.

It is also interesting to compare some of these results (obtained from a Faraday
rotation analysis) with those of O. K. Garriott et al. (22) (obtained from an analysis of
satellite doppler data) since some of their results refer to 1962 when solar activity was
approaching a minimum value ($R_g = 40$). In Table 3 the summer, winter and equinox
midday result obtained in 1962 by Garriott are shown together with summer, winter, and
equinox daytime results obtained in 1964 and 1965 by means of the Randle Cliff Radar.
We see at once that values of mean slab thickness and mean temperature (Garriott notes
that $T = (\overline{T_e} + T_i)/2$ in the absence of thermal equilibrium) are greater during 1964-65
than during the 1962 period, but values of mean total electron content are slightly less
during 1964-65 than those in 1962. The fact that total content is less in 1964-65 than in
1962 is hardly newsworthy since it would naturally be expected as a consequence of
diminishing solar flux. The fact that slab thickness and temperature are greater during
1964-65 than in 1962 is rather interesting. If one assumes that the 1962 results are
accurate, it follows that the ionosphere becomes warmer with decreasing solar activity,
which contradicts the notion that the ionospheric temperature should decrease under that
condition. The fact that midday results were considered in the 1962 analysis and entire
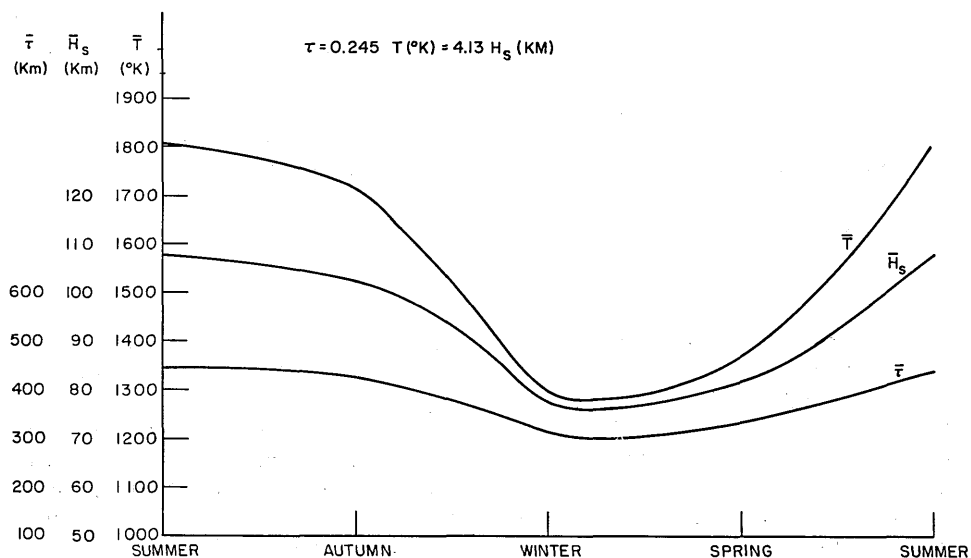
$\bar{\tau} = 0.245\ T(^\circ K) = 4.13\ H_s\ (KM)$

Fig. 12 – Seasonal variations of mean slab thickness $\bar{\tau}$, scale length $\bar{H}_s$, and neutral gas temperature $\bar{T}$

Table 3
Comparison of 1962 Results Obtained by Garriott
with 1964-65 Results Obtained by NRL

Season	Mean Slab Thickness $\bar{\tau}$ (km)		Mean Electron Content $\bar{C}$ (m^{-2})		Mean Temperature $\bar{T}$ (°K)		NRL Probable Error (%)
	Garriott 1962	NRL	Garriott 1962	NRL	Garriott 1962	NRL	
Summer	327	442	15×10^{16}	14.2×10^{16}	1337	1801	24
Autumnal Equinox		422		13.8×10^{16}		1717	32
Avg. Equinox	299	402	20×10^{16}	13.7×10^{16}	1220	1633	23
Vernal Equinox		335		11.0×10^{16}		1364	15
Winter	276	316	16×10^{16}	13.2×10^{16}	1125	1296	17
Yearly Avg.		387		13.0×10^{16}		1582	19

daytime results were considered in the 1964-65 analysis would tend to make the contradiction even more pronounced. (Unfortunately, if the NRL data were partitioned such that only midday values be considered, the results would not be statistically significant.) A primary cause of error could be a consequence of the inherent overestimation in the Faraday analysis due to the neglect of horizontal gradients. (The fact that horizontal gradients existed may be concluded here if the NRL results are truly overestimates.)

It has been calculated that overestimation may be as much as 25 percent at around 1500 EST. This is a consequence of the maximum north-to-south gradient of the $\bar{\psi}$ function and the maximum north-to-south gradient in electron content which exists during midafternoon. (Recall that all gradients in electron content are neglected in order to avoid the $n\pi$ rotational ambiguity.) In general the fractional error is given by

$$\frac{\delta C}{C_{i,f}} = \frac{1}{C_{i,f}} \left(\frac{d\,C/dt}{d\bar{\psi}/dt} \right) \bar{\psi}_{f,i} \, , \tag{6}$$

where δC is the error in the content, $C_{i,f}$ is the electron content at the initial or final point of the record, and $\bar{\psi}_{f,i}$ is the magnetic field parameter at the final or initial point. The numbers dC/dt and $d\bar{\psi}/dt$ are the average slopes of C and $\bar{\psi}$ over the transit, or portion of the transit, considered. Even though the absolute values of the slab thickness, total content, and neutral gas temperature may be overestimations of the true values, it is statistically evident that seasonal comparisons would not be affected appreciably. This may be verified through comparison with the results of Garriott et al. For instance they found in 1962 that the ionosphere was warmer in summer than in winter; this was also concluded from the NRL analysis. In general they found that the wintertime content was greater than the summertime content for large R_z, but these values tend to converge as R_z decreases. At $R_z = 40$ the seasonal averages intersect, and by extrapolation of the data one might expect the summertime content to be greater than the wintertime content for very low R_z. We see that this is the observed tendency of the NRL results — which amounts to a Faraday analysis verification of Garriott's doppler results for sunspot minimum.

CONCLUDING REMARKS

Faraday rotation studies at a single vhf frequency suffer due to the presence of horizontal gradients in the ionospheric electron content since Bowhill's fade rate analysis must be used. The utility of the fade rate procedure has been demonstrated, but in some instances large fractional errors might be expected to occur, especially during the midafternoon. Several methods have been suggested to remove the $n\pi$ rotational ambiguity and are worthy of consideration. The method which probably holds the greatest promise relies on the concept of utilizing two widely spaced frequencies. The upper frequency, being generally unambiguous, is used to obtain a coarse measure of the content in order to remove the rotational ambiguity of the lower frequency, which is used as a fine-scale measure. The concept is certainly not novel (it was probably first suggested by F. B. Daniels (26) but it has not been used extensively in radar application for the purpose of ionospheric investigation. The best combination of vhf and uhf frequencies should be governed by several factors. The vhf should be low enough to obtain fine resolution and yet be compatible with the high-frequency approximation, and the uhf should be high enough to render the rotation angle unambiguous. One is also restricted by a finite reading error at uhf. Suppose, for example, that the polarization of an incoming signal can only be established to within ζ at uhf. In order that the process of ambiguity removal at vhf not be confused, it follows that

$$\left(\frac{f_{uhf}}{f_{vhf}} \right) < \left(\frac{90}{\zeta} \right)^{1/2} \, ,$$

where ζ is the reading error in degrees and f is the radar frequency. If one requires precision such that vhf = 60 Mc/s, then for a nominal reading error of 5 degrees, the uhf must be on the order of 240 Mc/s. However, a value of 240 Mc/s is not high enough to render polarization unambiguous in most cases. Consequently, one must sacrifice at the vhf end and accept less precision in the fine-scale measure of content. It turns out that a vhf:uhf ratio of 1:4 is about optimum, with the uhf in the 400 to 500 Mc/s band. Although these were not necessarily the prime considerations, a vhf-uhf radar capability is being incorporated into the Randle Cliff 150-ft dish installation. The vhf is 138.6 Mc/s and the uhf will be 435 Mc/s.

ACKNOWLEDGMENTS

REFERENCES

1. Evans, J.V., "The Measurement of the Electron Content of the Ionosphere by the Lunar Radio Echo Method," Proc. Phys. Soc. (London), Ser. B, 69:953-955 (1956)

2. Hill, R.A., and Dyce, R.B., "Some Observations of Ionospheric Faraday Rotation on 106.1 Mc/s," J. Geophys. Res. 65:173-176 (1960)

3. Bauer, S.J., and Daniels, F.B., "Measurements of Ionospheric Electron Content by the Lunar Radio Technique," J. Geophys. Res. 64:1371 (1959)

4. Millman, G.H., Sanders, A.E., and Mather, R.A., "Radar-Lunar Investigations at a Low Geomagnetic Latitude," J. Geophys. Res. 65:2619 (1960)

5. Blevis, B.C., "Ionospheric Studies by the Lunar Radar Technique," Nature, 180:138 (1957)

6. Goodman, J.M., "Radar Measurement of the Cislunar Electron Content," (Paper presented to the NRL Electronic Council, Feb. 6, 1964)

7. Merrill, R.G., Lawrence, R.S., and Roper, N.J., "Synoptic Variations and Vertical Profiles of Large-Scale Ionospheric Irregularities," J. Geophys. Res. 68:5453 (1963)

8. Little, C.G., and Lawrence, R.S., "The Use of Polarization Fading of Satellite Signals to Study the Electron Content and Irregularities in the Ionosphere," J. Research Natl. Bur. Standards 64D:335 (1960)

9. Mechtly, E.A., and Rodrique, F.A., "Comparison of Winter Ionosphere Electron Contents Observed at Boulder, Stanford, Urbana and Huntsville," (paper presented at Spring 1963 URSI meeting, Washington, D.C.)

10. Argence, E., and Rawer, K., "Electron Density Profile Above the F2 Peak from Faraday Records," Proc. Third Int. Space Science Symp., COSPAR, 1962; pp. 230-46, New York:Interscience Publishers, 1963

11. Garriott, O.K., "The Determination of Ionospheric Electron Content and Distribution from Satellite Observation," J. Geophys. Res. 65:1139 (1960)

12. Yeh, K.C., and Swenson, G.W., Jr., "Ionospheric Electron Content and its Variations Deduced from Satellite Observations," J. Geophys. Res. 66:1061 (1961)

13. Dyce, R.B., "Faraday Rotation Observations of the Electron Content of the Exosphere," J. Geophys. Res. 65:2617 (1960)

14. Blackband, W.T., Burgess, B., Jones, I.L., and Lawson, G.J., "Deduction of Ionospheric Electron Content from the Faraday Fading of Signals from Artificial Earth Satellites," Nature, 183:1172 (1959)

15. Roger, R.S., "Some Ionospheric Measurements Using the Faraday Effect in Satellite Transmissions at 108 Mc/s," in "Radio Astronomical and Satellite Studies of the Atmosphere," pp. 325-332, Jules Aarons, ed., Amsterdam:North-Holland (1963)

16. Taylor, G.N., "Measurements of the Electron Content of the Ionosphere During Some Magnetically Disturbed Periods in Winter," J. Atmospheric Terrest Phys. 27:735 (1965)

17. Potts, B.C., "Mean Ionospheric Scale Heights Deduced from Faraday Rotation Measurements," J. Geophys. Res. 70:2651 (1965)

18. Ross, W.J., "The Determination of Ionospheric Electron Content from Satellite Doppler Measurements," J. Geophys. Res. 65:2601 (1960)

19. Munro, G.H., "Diurnal Variations in the Ionosphere Deduced from Satellite Radio Signals," J. Geophys. Res. 67:147 (1962)

20. Kelso, J.M., "Doppler Shifts and Faraday Rotation of Radio Signals in a Time-Varying, Inhomogeneous Ionosphere," J. Geophys. Res. 66:1107 (1961)

21. Garriott, O.K., and Nichol, A.W., "Ionospheric Information Deduced from the Doppler Shifts of Harmonic Frequencies from Earth Satellites," J. Atmospheric Terrest Phys. 22:30 (1961)

22. Bhonsle, R.V., da Rosa, A.V., and Garriott, O.K., "Measurements of the Total Electron Content and the Equivalent Slab Thickness of the Midlatitude Ionosphere," J. Research Natl. Bur. Std. 69D:929 (1965)

23. Nyberg, W.C., Kaiser, R.L., and Leavitt, W.E., "Experiments to Determine Communication Capability of Echo II Satellite," (paper presented at Int. Conv. on Military Electronics, Washington, D.C., 1964)

24. Goodman, J.M., "Prediction of Faraday Rotation Angles at VHF and UHF," NRL Report 6234, 1965

25. Seddon, J.C., "A Model of the Quiet Ionosphere," J. Geophys. Res. 68:1339 (1963)

26. Daniels, F.B., "Electromagnetic Propagation Studies with a Satellite Vehicle," in "Scientific Uses of Earth Satellites," pp. 276-282, J. A. Van Allen, ed., Ann Arbor: U. of Michigan Press, 1956

DOCUMENT CONTROL DATA - R&D

(Security classification of title, body of abstract and indexing annotation must be entered when the overall report is classified)

1. ORIGINATING ACTIVITY *(Corporate author)*	2a. REPORT SECURITY CLASSIFICATION
U.S. NAVAL RESEARCH LABORATORY WASHINGTON, D.C. 20390	UNCLASSIFIED
	2b. GROUP

3. REPORT TITLE

IONOSPHERIC PARAMETERS DERIVED FROM ECHO II RADAR RETURNS
DURING SOLAR MINIMUM CONDITIONS

4. DESCRIPTIVE NOTES *(Type of report and inclusive dates)*

An interim report on one phase of the problem

5. AUTHOR(S) *(Last name, first name, initial)*

Goodman, John M.

6. REPORT DATE	7a. TOTAL NO. OF PAGES	7b. NO. OF REFS
February 21, 1966	22	26

8a. CONTRACT OR GRANT NO.	9a. ORIGINATOR'S REPORT NUMBER(S)
NRL Problem R02-05	
b. PROJECT NO.	NRL Report 6375
RF 001-02-41-4001	
c.	9b. OTHER REPORT NO(S) *(Any other numbers that may be assigned this report)*
d.	None

10. AVAILABILITY/LIMITATION NOTICES

Distribution of this document is unlimited. Copies available from the Clearinghouse for Federal Scientific
and Technical Information (CFSTI), Springfield, Va., 22151

11. SUPPLEMENTARY NOTES	12. SPONSORING MILITARY ACTIVITY
None	Dept. of the Navy (Office of Naval Research), Washington, D.C.

13. ABSTRACT

Radar returns from the Echo II satellite (1964-4A) have been analyzed for Faraday rotation effects in order to ascertain their utility in deducing both the subsatellite electron content and the equivalent slab thickness of the daytime ionosphere. These two ionospheric quantities were computed for each satellite transit upon consideration of the Faraday fading phenomenon and the geomagnetic field parameter $H \cos \theta \sec X$. The analysis may lead to a possible overestimation of the electron content and slab thickness values, but the degree of overestimation should have only minor bearing on the relative effects. As a result of the present investigation, the following conclusions have been reached:

a. The subsatellite electron content generally exhibits a large variance, but its average value tends to be largest near midday and decreases with increasing solar zenith angle.

b. The daily equivalent slab thickness exhibits no marked variation between 0800 and 1800 EST, although midafternoon values are somewhat in excess of prenoon values.

c. The seasonal equivalent slab thickness has its minimum in local winter and its maximum in local summer; the equinox values are intermediate, with the autumnal equinox exhibiting higher computed values than the vernal equinox period.

d. The mean scale height $\overline{H_s}$ and the mean neutral gas temperature $\overline{T}$ for the ionosphere were found to be 94 km and 1582°K, respectively, during daytime hours. The daytime ionosphere was found to be 500°K warmer in summer than in winter, with the mean equinox temperature being close to the all-season average.

e. No pronounced correlation with Zurich sunspot number or decimetric solar flux was discernible, which was probably due to the fact that statistical variations in the observations exceeded the real variations which might have occurred as a result of solar activity changes.

f. No correlation with the magnetic index K was noted.

These conclusions are based on radar echo data obtained during the recent period of minimum solar activity.

14. KEY WORDS	LINK A		LINK B		LINK C	
	ROLE	WT	ROLE	WT	ROLE	WT
Ionosphere						
Electron Content						
Slab Thickness (Ionosphere)						
Magneto-Optic Effect						
Ambiguity Removal (Magneto-Optic)						
Very High Frequency						
Radar Reflections						
Echo II (Artificial Satellite)						
Moon						

INSTRUCTIONS

1. ORIGINATING ACTIVITY: Enter the name and address of the contractor, subcontractor, grantee, Department of Defense activity or other organization (corporate author) issuing the report.

2a. REPORT SECURITY CLASSIFICATION: Enter the overall security classification of the report. Indicate whether "Restricted Data" is included. Marking is to be in accordance with appropriate security regulations.

2b. GROUP: Automatic downgrading is specified in DoD Directive 5200.10 and Armed Forces Industrial Manual. Enter the group number. Also, when applicable, show that optional markings have been used for Group 3 and Group 4 as authorized.

3. REPORT TITLE: Enter the complete report title in all capital letters. Titles in all cases should be unclassified. If a meaningful title cannot be selected without classification, show title classification in all capitals in parenthesis immediately following the title.

4. DESCRIPTIVE NOTES: If appropriate, enter the type of report, e.g., interim, progress, summary, annual, or final. Give the inclusive dates when a specific reporting period is covered.

5. AUTHOR(S): Enter the name(s) of author(s) as shown on or in the report. Enter last name, first name, middle initial. If military, show rank and branch of service. The name of the principal author is an absolute minimum requirement.

6. REPORT DATE: Enter the date of the report as day, month, year; or month, year. If more than one date appears on the report, use date of publication.

7a. TOTAL NUMBER OF PAGES: The total page count should follow normal pagination procedures, i.e., enter the number of pages containing information.

7b. NUMBER OF REFERENCES: Enter the total number of references cited in the report.

8a. CONTRACT OR GRANT NUMBER: If appropriate, enter the applicable number of the contract or grant under which the report was written.

8b, 8c, & 8d. PROJECT NUMBER: Enter the appropriate military department identification, such as project number, subproject number, system numbers, task number, etc.

9a. ORIGINATOR'S REPORT NUMBER(S): Enter the official report number by which the document will be identified and controlled by the originating activity. This number must be unique to this report.

9b. OTHER REPORT NUMBER(S): If the report has been assigned any other report numbers (either by the originator or by the sponsor), also enter this number(s).

10. AVAILABILITY/LIMITATION NOTICES: Enter any limitations on further dissemination of the report, other than those imposed by security classification, using standard statements such as:

(1) "Qualified requesters may obtain copies of this report from DDC."

(2) "Foreign announcement and dissemination of this report by DDC is not authorized."

(3) "U. S. Government agencies may obtain copies of this report directly from DDC. Other qualified DDC users shall request through
_____ ."

(4) "U. S. military agencies may obtain copies of this report directly from DDC. Other qualified users shall request through
_____ ."

(5) "All distribution of this report is controlled. Qualified DDC users shall request through
_____ ."

If the report has been furnished to the Office of Technical Services, Department of Commerce, for sale to the public, indicate this fact and enter the price, if known.

11. SUPPLEMENTARY NOTES: Use for additional explanatory notes.

12. SPONSORING MILITARY ACTIVITY: Enter the name of the departmental project office or laboratory sponsoring (paying for) the research and development. Include address.

13. ABSTRACT: Enter an abstract giving a brief and factual summary of the document indicative of the report, even though it may also appear elsewhere in the body of the technical report. If additional space is required, a continuation sheet shall be attached.

It is highly desirable that the abstract of classified reports be unclassified. Each paragraph of the abstract shall end with an indication of the military security classification of the information in the paragraph, represented as (TS), (S), (C), or (U).

There is no limitation on the length of the abstract. However, the suggested length is from 150 to 225 words.

14. KEY WORDS: Key words are technically meaningful terms or short phrases that characterize a report and may be used as index entries for cataloging the report. Key words must be selected so that no security classification is required. Identifiers, such as equipment model designation, trade name, military project code name, geographic location, may be used as key words but will be followed by an indication of technical context. The assignment of links, roles, and weights is optional.